Technische Universiteit
Eindhoven
University of Technology

Department of Mechanical Engineering

Design and Preliminary Validation of an EMG-driven Control Strategy for a Twisted String Actuated Elbow Flexion Assistive Device

Internship at University of Bologna

DC 2017.038

F.J.M. Heck 0814199

Supervisors:
Eng. R. Meattini
Prof. G. Palli
Prof. C. Melchiorri

Reviewer:
Prof. dr. H. Nijmeijer

Eindhoven, April 1, 2017

Abstract

One area of technological healthcare focuses on the rehabilitation of muscles by applying robotic devices on the human body, such as exoskeletons. With the Twisted String Actuated (TSA) module the elbow joint is assisted using an electromyography (EMG) driven control strategy for a lifting task to limit the muscle activity. Since advanced modeling techniques are often inaccurate and because the human interaction is hard to model, a more direct EMG-driven control strategy is proposed. The control parameters can easily be set by means of two small calibration experiments, ensuring a high adaptability to different users. An experiment, containing a calibration and an execution phase, shows that the control strategy is able to limit the EMG activity of the subject during the lifting task. Using the TSA module creates new possibilities to assist the muscles of the human body.

List of Symbols

Symbol	Quantity	Unit	Notation
b	Damping coefficient	Newton second per meter	Nsm^{-1}
F	Force	Newton	N
k	Stiffness	Newton per meter	Nm^{-1}
L	Length	meters	m
r	Radius	meters	m
t	Time	seconds	s
x	Position	meters	m
α	Angle	degrees	$^{\circ}$
θ	Angle	radians	$-$
τ	Time	seconds	s

Contents

1 Introduction

In the last couple of decades a lot of research has been done to improve healthcare by use of technology. A specific area of this technological healthcare focuses on the rehabilitation of muscles, by interaction between robotic devices and the human body. An example of these robotic devices are so called exoskeletons, that provide supporting forces or torques using motors that are attached to an external skeleton. The exoskeleton can often be worn, like in [1], [2] and [3]. These exoskeletons are designed for the upper arm, though like some other exoskeletons, require an additional frame.

The exoskeleton control methods can mainly be divided into two groups. The most common method of control is to use advanced models to estimate the joint torques that are needed to perform the movement. By making use of a common fraction of the torque that is estimated as an assistance torque, the muscle activation of the user can be reduced, since the human motor behavior will adapt to the applied support. This common fraction is often set by the user, as in [4], whereas a more general calibration would be preferable. However, the advanced modeling approach has two main drawbacks. It is very difficult to determine accurately the joint torques that are required in real-time and the reaction of the user to the support cannot be properly modeled. One possibility for the torque estimation is using inverse dynamics, but this requires an accurate dynamic model of the limb, which is user dependent and therefore often impractical.

Another group of approaches utilizes a newer area of research, using the biological signals from the human body. Since some movements are generated in the brain, some in the brain stem and some in the spinal cord, the signals can best be recorded at the peripheral nervous system, measuring the activity of muscle fibers, activated by motor neurons. The electromyography (EMG) signals can be measured in two ways: with invasive (needle) electrodes or non-invasive (surface) electrodes. The EMG-approach has some advantages: according to [5], the signal is transmitted about 20-80 ms before the muscle contracts. This delay can be used to assist the muscle before the movement occurs, or even help in the start-up phase of the movement. The non-invasive surface EMG (sEMG) electrodes are used in this research, as they are more appropriate for recording human motion detection, as no surgical constraints are imposed.

Disadvantages of the EMG-approaches are mainly related to the signal acquisition and user-specific calibration. The EMG-signal is affected by the condition of the skin, as well as the position of the electrode and the amount of muscle fatigue. Therefore, the EMG-based controllers will need custom calibrations, both for different users as for different sessions with the same user.

EMG-methods can be divided into multiple control methods, such as neuro-fuzzy controllers like in [6], neurological controllers like in [7], proportional controllers as used in [4] and the hill-type muscle model as in [8]. In general, the complex physiological models achieve a higher accuracy, though they also have a lot of parameters that are subject-dependent. Therefore, a long calibration time is needed, which is not desirable.

In this research the muscle activity will be limited to a known threshold during a lifting task, by using the Twisted String Actuated (TSA) Module as the assistance device [9]. The TSA module uses a small DC-motor to twist strings, applying a force on the end of the string in the process. The module is designed to actuate in a rapid way, while being lightweight. This way the assistive device does not need an additional frame and can be attached to the subject directly. A goal for this project is to limit the EMG activity during a lifting task, as EMG has only been reduced in literature, but not limited. Since one focus of the use of the assistance is at rehabilitation, the used control should be easily adaptable to different users, because long calibration phases are undesired for use in professional rehabilitation clinics.

In Chapter 2 more information will be given about the working principle behind muscles and their electrical signals. The TSA module will be discussed in further detail in Chapter 3. In this research the muscle activity will be limited to a predetermined EMG value. A simple calibration experiment is used in order to effectively limit the EMG. Another experiment has been executed for different subjects to show the robustness of the control strategy. The calibration experiment and the control strategy will be explained in Chapter 4. The experimental evaluation of the proposed strategy is presented in Chapter 5. Final conclusions and recommendations for future work are given in Chapter 6.

2 EMG

In this chapter the muscle working principle is briefly described with information from [10]. First the mechanics behind muscles are explained, after which the EMG signal measurement and processing are presented.

2.1 Muscle Mechanics

Muscles consist of controllable motor units which are controlled by a motor axon. The motor units control the muscle fibers to make the muscle contract and vary its length to ensure movement or to apply forces on the joint the muscle is attached to with a tendon. Each muscle has a finite number of motor units, which are controlled by separate nerve endings. The muscles create tension by using the motor unit action potential, creating an electric signal: an electromyogram (EMG). The motor units fire off in stages. First the smallest motor units fire off. When a threshold is reached, a bigger set of motor units also starts to fire off, generating a higher tension. Tension reduction follows the reverse process: first the biggest motor units stop firing. The contraction time depends on the muscle, the person and the experimental technique. Typical turn on times are 200 ms and turn off times are 300 ms. There are several ways of modeling muscles, which are briefly explained in Appendix A.

2.2 EMG Signals

The EMG signals that are created to increase the tension in muscles and move them can be measured by EMG electrodes. The higher the force used by a muscle, the more motor units fire and the larger the amplitude of the EMG signal. The EMG signal is a superposition of the electric signals from every motor unit to the muscle fibers, as can be seen in Figure 2.1. The EMG electrodes can be divided into two groups: indwelling electrodes and surface electrodes.

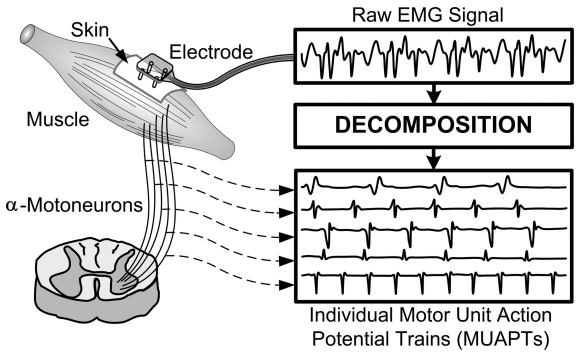

Figure 2.1: The raw EMG signal is a superposition of the electric signals from every motor unit to the muscle fibers. [11]

The indwelling EMG electrodes are required to measure smaller muscles and underlying muscles. The needle electrode is a fine needle with an insulated conductor inside. The fine-wire electrodes have the thickness of a human hair and require a needle to insert. After removing the needle, the wire remains inside in contact with the muscle. They measure not only the waves that are conducted in the surface, but also in a small area around the electrode. The indwelling electrodes measure a slightly different spectrum of the EMG signal, with the largest spectral density in the region between 20 and 400 Hz, where the surface EMG spectrum only has a concentrated signal up to 200 Hz.

The surface EMG (sEMG) electrodes consist of metal disks, usually silver or silver chloride, about 1 cm in diameter. These electrodes are placed on the skin above a muscle with a superconducting gel and measure an average activity of the muscle. The sEMG can be used to measure the larger muscles, which are located towards the skin. The sEMG electrodes measure a larger area of the

muscle, containing more motor units and resulting in a signal of higher amplitude. The sEMG spectrum is most concentrated in the range between 20 and 200 Hz. For the deeper muscles, indwelling EMG electrodes should be used, since otherwise a lot of cross-talk will be measured. Cross-talk is the measurement of EMG signals of multiple muscles at once, resulting in undesired noise.

2.3 EMG Processing

The EMG signals can be processed using different techniques. The most common techniques combine the following things. The absolute value of the signal is taken to show the magnitude of the signals. Next, a low-pass filter can be used to smoothen the signal. Some techniques also involve integrating the signal. This is used in different ways, from triggering every fixed amount of time to triggering by a threshold value of the integrated signal.

By using two sEMG electrodes, placed next to each other, common noise can be removed by subtracting the two signals. Furthermore a larger disturbance is measured from the power line hum, which is at 50 Hz. This can be easily removed by using a notch filter. Also movements, which are in the 0-10 Hz range, can disturb the signal. Since the EMG spectrum is mostly in the range between 20 and 200 Hz, with components up to 1000 Hz, the movement disturbance can best be filtered by using a 20 Hz high-pass filter. An amplifier should be used to increase the strength of the EMG signals, as they are have a maximum amplitude up to 5 mV.

During the project sEMG has been used, since the sEMG has been shown more reliable than the indwelling EMG and the number of motor units in the pick-up zone is considerably larger. Also applying the sEMG is easier. The sEMG is measured using sEMG electrodes, which are connected to an electric board that sends the data using Bluetooth to the desktop. The electric board used is made by the Electrical Engineering faculty of the University of Bologna. The raw sEMG signal is processed using the scheme of Figure 2.2. First a 50 Hz notch filter and a 20 Hz high pass filter reduce the noise. From this signal the Root Mean Square (RMS) value is taken, as the amplitude of the signal contains information about the muscle activity.

Figure 2.2: The sEMG signal processing.

As can be seen in Figure 2.3, more information can be gathered from the filtered signal. When the muscle contracts, more motor units fire off, increasing the measured EMG signal amplitude. In the filtered signal this can be read off in more detail, whereas the raw signal looks like noise with increasing amplitude. The filtered signal is therefore used in the control strategy of Chapter 4.

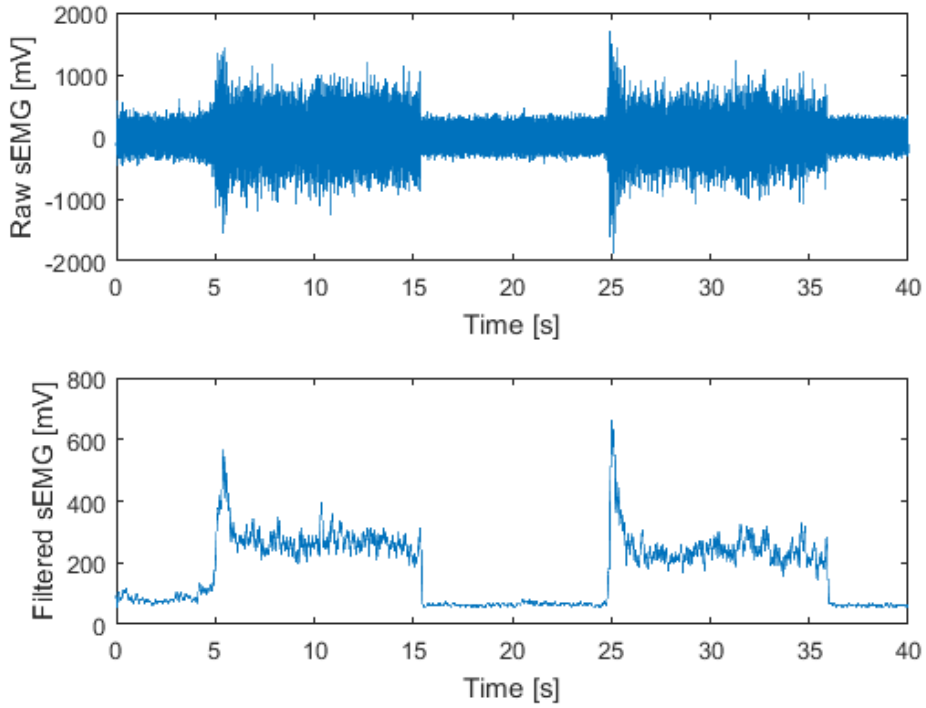

Figure 2.3: The raw and filtered sEMG signal.

2.4 Conclusion

In this chapter the working principle of the muscles is explained, as well as the gathering of relevant data from the muscle activity using EMG. During the project sEMG is used and filtered as stated above. This filtered EMG can be used in the control strategy of Chapter 4. In the next chapter the actuator module is explained, which is also needed to be able to apply the control strategy on the system.

3 TSA Module

In this chapter the concept of the twisted string is explained. The main components of the TSA module are summed, after which the control of the actuator is presented, along with some figures that illustrate the performance and stability.

3.1 Twisted String

Two or more strands are connected in parallel to a rotary DC motor on one end and to the fixation at the arm on the other end. The twisting of the strands results in a decrease in length of the transmission, allowing a force to be transmitted. In Figure 3.1 the string length for string twisting of a 50 mm long string is shown. The schematic overview of the TSA module is given in Figure 3.2.

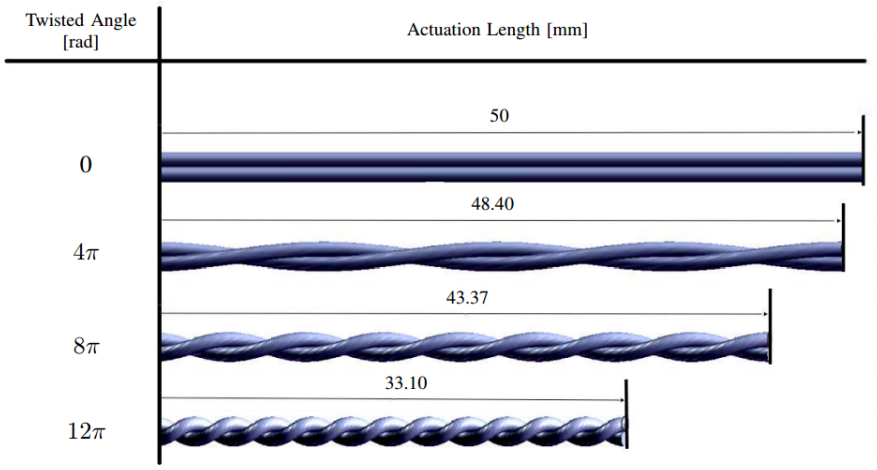

Figure 3.1: Twisted string concept. [12]

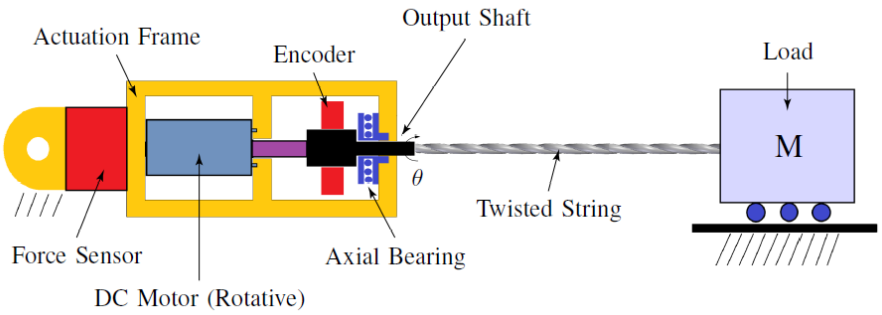

Figure 3.2: Schematic representation of the TSA module. [9]

In the schematic representation the twisted string is fixed to the module on one end and to the load on the other end. The string is attached to the module using a needle with a barb. A small plastic cylinder is placed on the needle to ensure that the strings will not come loose while twisting. The fixation to the load is in this project a fixation to the lower arm.

The high reduction ratio of the transmission allows the use of a small DC motor. The reduction ratio is related to the number of strands and the strand radius, which is further described in [12]. The string length L_s can be determined for every measured angle in sensor slots θ_{twist}. The rotation sensor counts 20 slots per rotation. The string length L_s is determined as follows

$$L_s(\theta_{twist}) = \sqrt{(L_0 + L_1 cos(\theta_0))^2 - (\theta_{twist}\frac{\pi}{10})^2 r^2}, \tag{1}$$

with r the strand radius and θ_0 the measured elbow angle in stretched position of the arm. L_0 is the distance between the elbow and the TSA module and L_1 is the lower arm length, which are both calculated from the string lengths in the two measured elbow positions; where the arm is stretched and where the elbow is bent, according to the schematic overview of Figure 3.3.

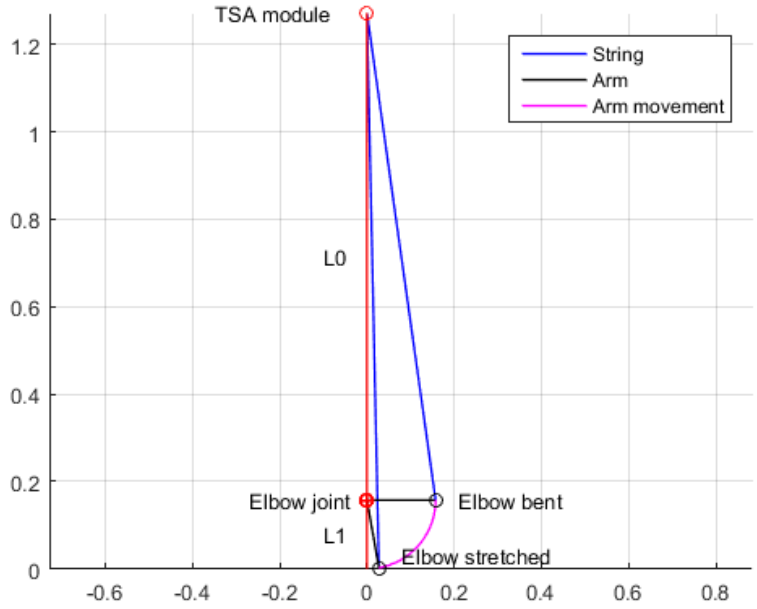

Figure 3.3: Schematic overview of twisted string variables.

Using the string length at any position of the DC motor, the elbow angle α can be estimated during the movement as follows

$$\alpha = \frac{180}{\pi} \arccos(\frac{L_s + L_a - L_0}{L_1 + L_a}). \tag{2}$$

Here L_a is the length of the attachment device, measured from the attachment of the string to the arm. The elbow angle estimation is only used to illustrate when the movements occur, as the accuracy was not very high due to slip in the soft connection from the TSA module to the string when moving the arm downwards at higher velocities.

The string that is used during experiments in this project has a length of 1.25 m to make sure there would be no undesired behavior, such as rolling up of the string, during the movement of the arm. The use of this long string requires a fixation of the TSA module on the back of the user, as suggested in Figure 3.4. This fixation would cause an extra bending of the string, which might partially change the behavior of the string twisting, but this behavior is neglected during this project as that situation was being researched at the university during the project.

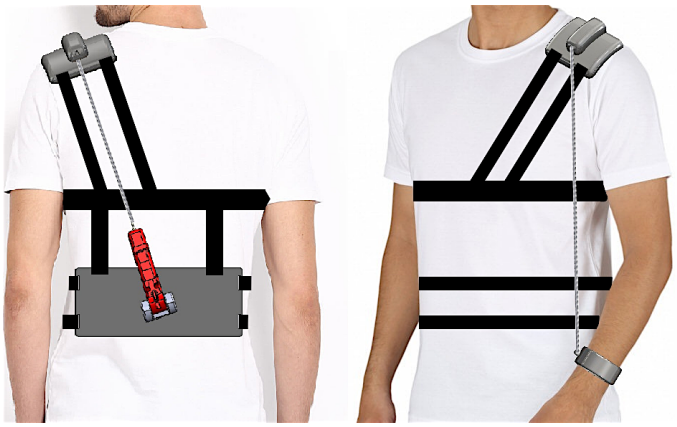

Figure 3.4: Concept of fixation of the TSA module at the back of the user.

3.2 Module

The TSA module is a small and lightweight module, designed by M. Hosseini et al. [9]. The module contains a DC motor, force sensor based on optoelectronic components and a rotational encoder. The module is connected to an Arduino NANO board, which is used for the control of the actuator and the acquisition of the signals from the force sensor and the rotational encoder. The force sensor can measure forces up to 100 N, with a resolution of 0.98 N. The rotational sensor measures 20 slots per rotation. The module can be connected to a wearable supporting frame by use of a bolt or a rod at the location shown in the Figure 3.5. The detailed view of the components of the TSA module is also given in this figure.

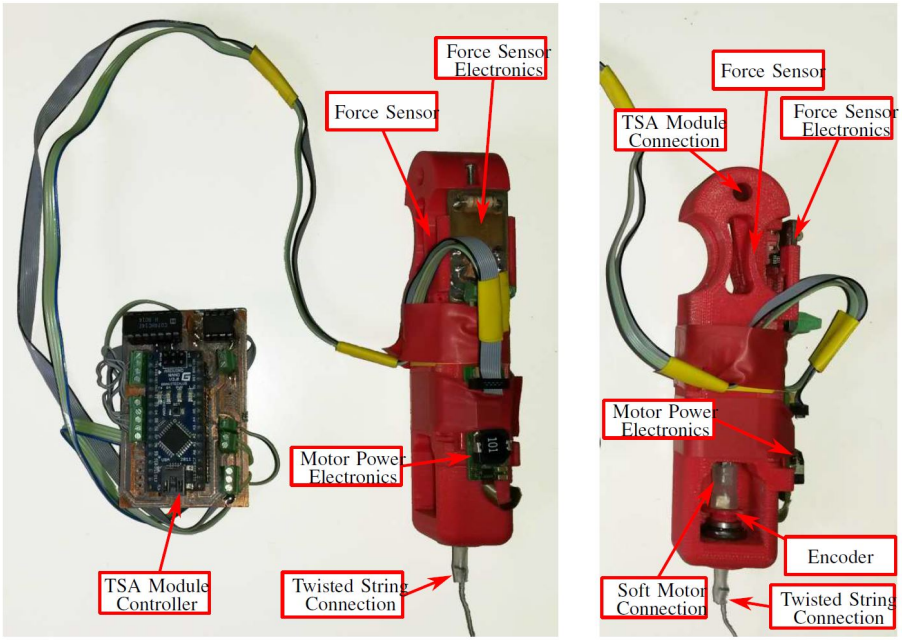

Figure 3.5: Detailed view of the TSA module. [9]

3.3 TSA Control

To properly actuate the twisted string using the TSA module, first the controller needed to be tuned. For this project a force control has been used, which is created with a feedback loop in Simulink, using the measured force of the force sensor in this loop (see Appendix B. To tune the controller, an experimental setup has been made where the TSA module is fixed to a solid frame

and the twisted string is fixed to the world to be able to properly use the force sensor. First a plant estimation is obtained, using the three-point method. The obtained signals are sampled at 100 Hz and windowed with a Hann window with an nfft of 400. The plant estimation is given in Figure 3.6a. The Process Sensitivity coherence is shown in Figure 3.6b. From this can be concluded that the plant estimation is usable between about 0.4 and 2.0 Hz. Above 2 Hz the coherence decreases, first due to the anti-resonance, lowering the magnitude of the signal. After 2 Hz the coherence remains low due to the noise, created partially by the allowed rotational movement of the TSA module at the fixation. Below 0.4 Hz the windowing causes for a lower coherence.

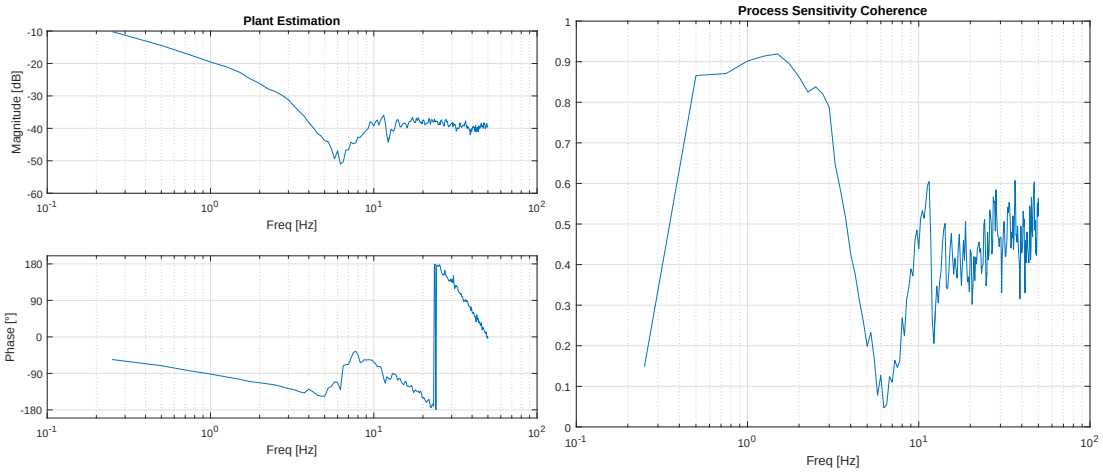

(a) Plant estimation.

(b) Process Sensitivity coherence.

Figure 3.6: Plant estimation and Process Sensitivity coherence.

Using loop-shaping, the controller has been tuned to be a PI-controller, with a proportional gain of 15 and an integral gain of 45. This results in the open loop estimation of Figure 3.7a and the Nyquist plot of Figure 3.7b.

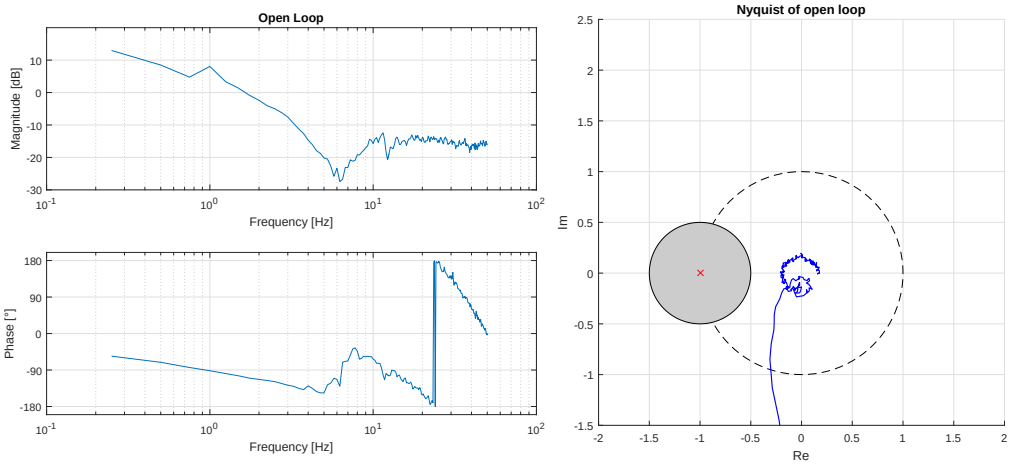

(a) Open loop estimation.

(b) Nyquist plot.

Figure 3.7: Open loop and Nyquist plots.

From the open loop plot the bandwidth can be determined, which is about 1.7 Hz. From the Nyquist plot the theoretical stability can be derived. A multi-step signal has been used to check if the system is stable and the performance is acceptable for the application, which can be seen in Figure 3.8.

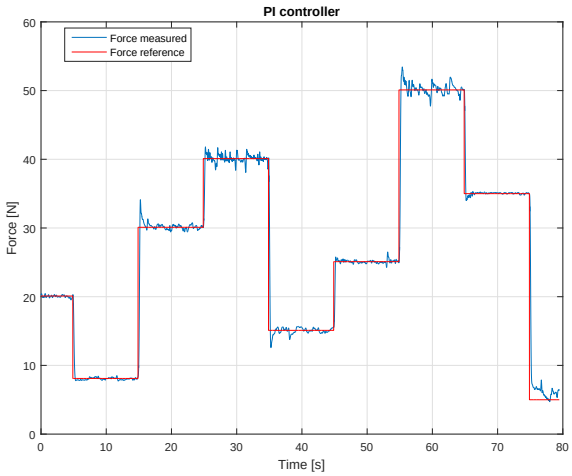

Figure 3.8: Multi-step response signal to check stability and performance.

From the multi-step response signal it can be seen that the controller should be stable. However, some overshoot can be seen. This amount of overshoot is acceptable, as no step responses will need to be followed when using the TSA module. Furthermore some room for increasing of the gains seems possible from the Nyquist plot for stability, but this was not possible due to the limitations of the DC-motor that was used as otherwise the input current limits would be reached. Also some noise can be seen in the constant section. One possible cause is the resolution of the force sensor, since the setpoints were not multiples of the resolution. The integrator then increases even when the setpoint is reached as closely as possible. Another reason is the slow response of the system, as the elasticity in the twisted string has influence on the force that is measured. At the end of the plot some undershoot is seen, which is caused by slip in the soft connection between the DC-motor and the twisted string. This causes for the string to remain twisted a couple of rotations after quickly untwisting the string to the starting untwisted position, where the workspace was limited for safety reasons. This results in a remaining rest force applied by the string, which is larger than the reference force.

3.4 Conclusion

In this chapter the twisted string concept is explained, as well as the components of the TSA module. After that the control of the TSA module is shown, which can be used further on in the project. In the next chapter the EMG-based control strategy is presented, combining both the EMG knowledge of Chapter 2 with the TSA module of this chapter.

4 EMG-driven Control Strategy

In this chapter the EMG-driven control strategy is presented. First the goal of the strategy is described, whereafter the controller is explained. The controller makes use of thresholds that are tuned semi-automatically, based on a calibration.

4.1 Setup

In this project the objective is to limit the muscle activity for a lifting task using the TSA module. This is done by using an EMG-driven control strategy. To show difference in muscle activity, the muscle activity is measured during a lifting task of a 2 kg load without support and a lifting task of a 2 kg load with support from the TSA module. The subject is seated on a chair, while the TSA module is fixed to the platform above him. The twisted string is fixed to the lower arm using the white connection device, as can be seen in Figure 4.1. The load is connected to the wrist using a strap. On the chair behind the subject the EMG acquisition device is located, which is connected to the desktop using Bluetooth and connected to the subject using the electrodes as mentioned in Chapter 2. The electrodes are placed on the biceps, since this is the main muscle for lifting the lower arm. This situation is shown in Figure 4.1, as well as the forces that play a role in the setup.

Figure 4.1: The experimental setup forces.

In the experimental setup from Figure 4.1, three forces can be seen: the muscle force F_{arm}, the load force F_L and the actuator force F_{TSA}. By setting the actuator torque equal to the load torque, the muscle force can be reduced, while remaining in control of the movement.

4.2 Controller

In Figure 4.2 the block diagram of the control system is shown. On the human arm two external forces are at work: one from the load and one from the actuator. The actuator force is determined using the EMG-driven control strategy, which makes use of the measured EMG and two thresholds. These thresholds are presented in more detail later. The controller that has been used in the control strategy is a PI controller, with a switching input according to the state of the EMG compared with the thresholds, as explained in the next section. The force that should be applied is applied

by the TSA module, with some error created by the TSA controller since the force control is not perfect.

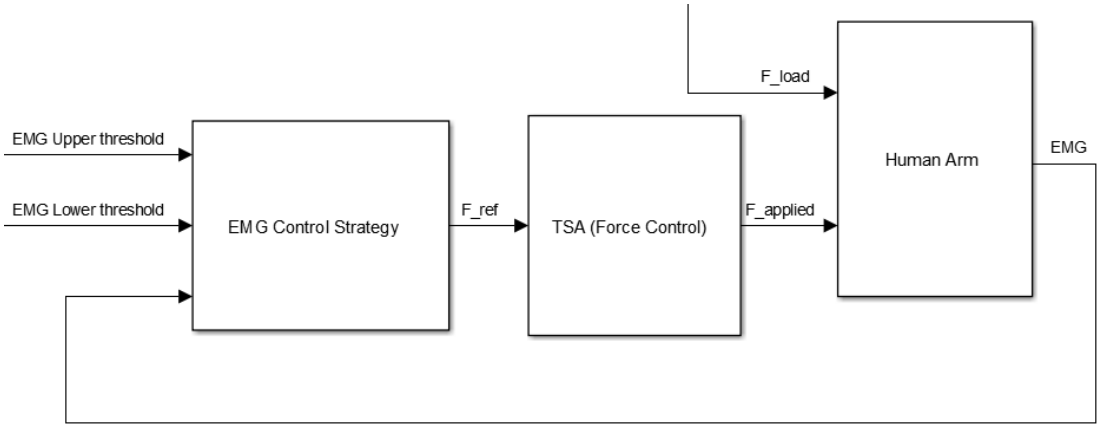

Figure 4.2: The block diagram of the control system.

4.3 Thresholds

The control strategy uses two thresholds, as seen in Figure 4.3: the EMG upper threshold and the EMG lower threshold. The threshold values are determined using a calibration, which is explained in the next section. The input to the proportional and the integral part of the controller is determined according to the thresholds.

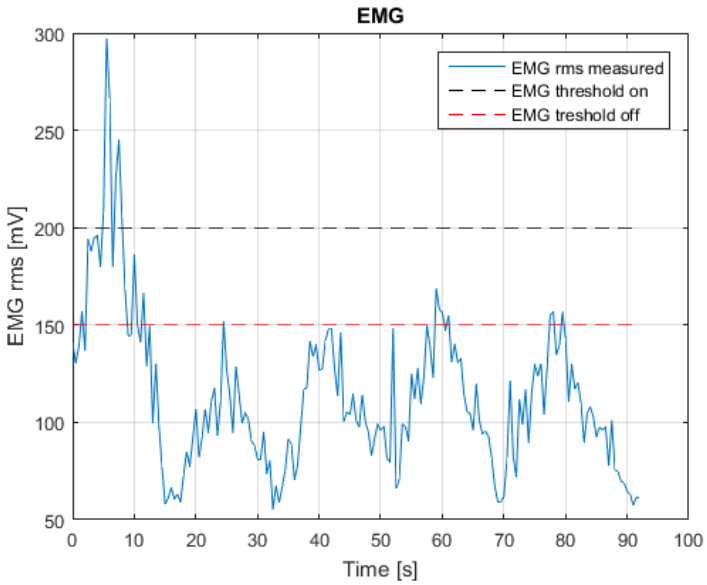

Figure 4.3: The upper and lower threshold.

When the measured EMG is above the upper thresholds for one full second, the controller input is activated, increasing the force assistance to lift the load. This force is partially 'memorized' in the controller, since the use of the integrator plays a significant role. The integral part will keep on increasing, according to the difference of the EMG compared with the lower threshold, until the EMG measured is under the lower threshold. From that moment the controller input is deactivated, leaving the integral action unchanged, until the EMG is above the upper threshold for one full second again. This would reactivate the controller input. This activation of the controller is shown in Figure 4.4.

The controller input is activated after one full second to filter out the behavior of the human body reacting on external influences, as this often resulted in larger peaks that would undesirably increase the force assistance.

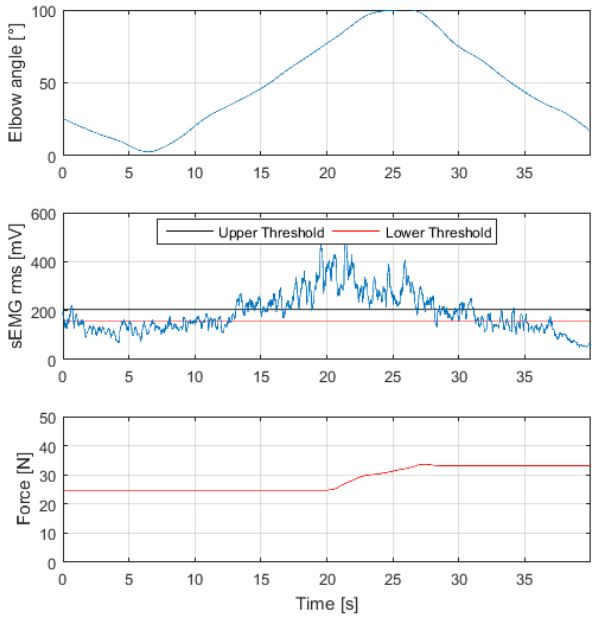

Figure 4.4: The activation of the controller using thresholds.

In the figure above the EMG starts increasing because of two reasons. First, the load moment increases on the muscle, as the arm of the moment increases. Second, the arm starts rotating around the elbow joint, changing the muscle length and increasing the EMG signal as well. After 13 seconds, the EMG starts increasing above the upper threshold. However, the EMG does not rise above the threshold for one full second, thus not (re)activating the controller input. At 20 seconds the control input is activated, increasing the assistance from the TSA module, which reduces the muscle force needed. This reduces the EMG measured. At about 27 seconds the measured EMG is under the lower threshold, deactivating the controller input and 'memorizing' the assistance force needed so it can be used as a starting assistance force for the next lifting iteration.

The gains of the controller are determined by performing a quick experiment, lifting the 2 kg load without support to determine the EMG values of the subject. This way the speed of the memorizing can be set, as a larger integral gain results in a fast increase of the memorizing effect. However, if the integral gain is set too large, the controller will assist with a too large force, making the stretching movement harder or impossible. Setting the proportional gain too large will result in a noisy control, as the input signal of the controller is the filtered EMG signal measured, which is still quite noisy. However, setting the proportional gain very low will result in a slow response to the measured EMG error.

4.4 Threshold Calibration

Since the EMG measurements are depending on subjects as well as sessions, some calibration should be applied for each subject and session to determine the thresholds properly. As the goal of the experiments is to limit the muscle activity during a lifting task to a fixed value, the chosen limit is the muscle activity of 0.5 kg. This way lifting 2 kg of load will sense like lifting 0.5 kg. The calibration of the thresholds therefore is done by lifting a 0.5 kg load in the upper position (90 degrees rotation around the elbow joint) for a longer period of at least 10 seconds. An example of this measurement is shown in Figure 4.5.

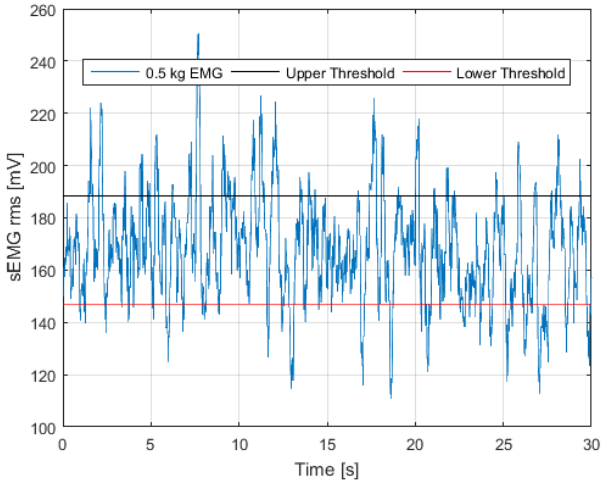

Figure 4.5: A calibration measurement for threshold determination.

From this calibration measurement the thresholds can be roughly determined by making use of the mean value and the standard deviation. Since the signal is quite noisy, the 68% confidence interval is used as an indication for the thresholds. The upper threshold is chosen as the mean value plus the standard deviation, where the lower threshold is the mean value minus the standard deviation. As mentioned, these values give an indication and are checked manually by analyzing the plot of the calibration measurement. This way an efficient calibration for the thresholds is achieved.

4.5 Conclusion

In this chapter the EMG-driven control strategy is explained using the knowledge of Chapter 2 and 3. The setup for the calibration experiments is shown, as well as the calibration of the thresholds that is needed to properly use the controller. In the next Chapter the EMG-driven control strategy will be tested with an experimental evaluation.

5 Experimental Evaluation

In this chapter the control strategy will be experimentally evaluated. First the experiment that is performed on four subjects is presented. This experiment consists of two parts: a calibration part and a testing part, which are performed right after each other. The results of these experiments are shown and analyzed. As the system has some limitations, these limitations are stated to be able to introduce some recommendations for future work.

5.1 Experiment

During the evaluation experiment of the control strategy, the same setup as in Chapter 4 is used, but with a different experimental approach. In Figure 5.1 the TSA module, string, connection and load are shown. For the experiment the 2 kg load is used.

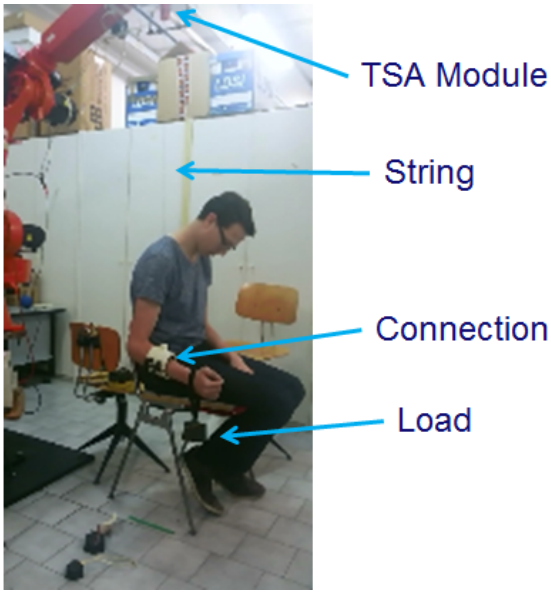

Figure 5.1: The experimental setup components.

The experiment is executed in two stages. First a calibration stage is executed to experimentally determine the required assistance force. The subject is asked to perform the lifting movement several times with a short break of 3 seconds when in the upper position (90 degrees rotation of the elbow joint). During this lifting movement the control strategy causes the controller input to be activated and deactivated, increasing the assistance force in the process. This way the support is gently increased, further reducing the muscle activity of the subject with each iteration. When the controller does not increase the supporting force anymore during a full iteration, the calibration phase is completed and the system is ready to be used.

The second part of the experiment starts right after the calibration phase is finished. In this part the subject is asked to lift the load several times, without a break in the upper position, to show that the EMG is limited to the upper threshold, giving the sensation of lifting 0.5 kg. If the calibration is performed correctly, the assistance force should be correct and the EMG should be limited to the set upper threshold. However, the controller is still active for two reasons. First, in case the calibration has not been fully successful, the controller should be adaptable to still increase the assistance force, reducing the force needed from the muscle. Second, this way the controller is adaptable for increasing loads; once the load is increased during the lifting, the muscle activity EMG will rise, increasing the need for more assistance.

5.2 Results

The experiment described above has been executed for four subjects. In this chapter the results of only one subject will be analyzed, along with some interesting phenomena, since the results of the other subjects are similar. The results of the other subjects are presented in Appendix C.

For subject A the calibration with the 0.5 kg load resulted in the thresholds from Figure 5.2. The EMG-driven controller has been tuned using the 2 kg experiment without assistance, as mentioned in Chapter 4. This resulted in a proportional gain of 0.001 and an integral gain of 0.03 to be used in the EMG-driven controller, applied on the difference between the measured EMG signal and the lower threshold.

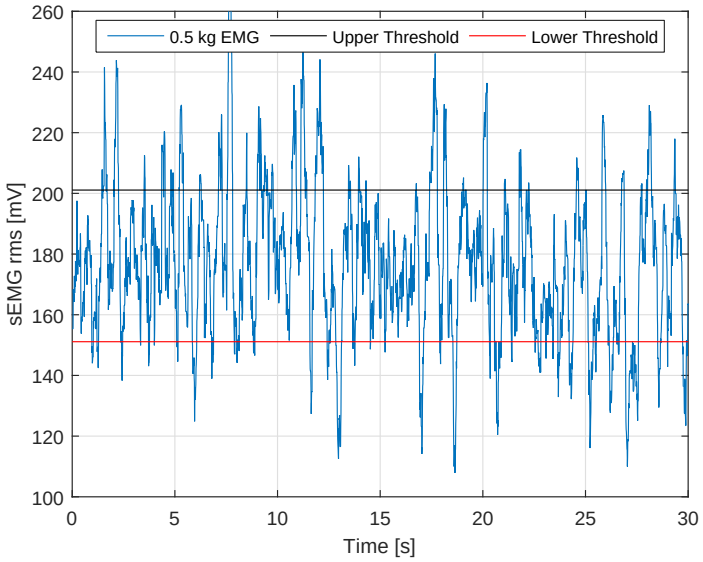

Figure 5.2: The thresholds for subject A, determined using the 0.5 kg load calibration experiment.

In the figure above it can be seen that the filtered EMG for a constant position shows quite some variations. These variations are one of the reasons to choose a switching controller, since the real time control needs to be influenced by the variations as little as possible. The use of thresholds to trigger the switching controller results in a proper solution for this problem.

Using these thresholds the experiment described in Section 4.4 is performed. The results of the experiment for subject A are shown in Figures 5.3 and 5.4. These figures each contain three graphs. The first graph shows the elbow angle estimation, as explained in Chapter 3. The second graph shows the measured EMG, as well as the thresholds. The last graph shows the assistance force that should be applied together with the measured force. Figure 5.3 shows the calibration phase, where Figure 5.4 shows the execution phase. The two phases are executed directly after each other, but are presented in different figures due to the long time intervals.

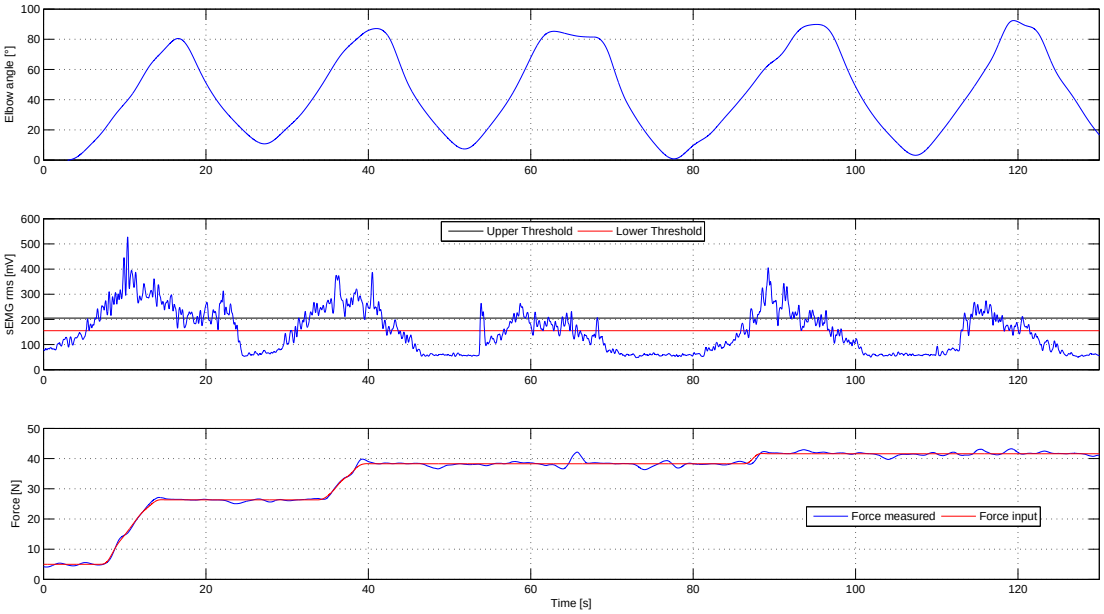

Figure 5.3: The calibration phase of the experiment for subject A.

In Figure 5.3 the calibration phase is shown, where the EMG is still over the upper threshold. The assistance force starts at 5 Newton to make sure the string is under tension during the movement. When the EMG has surpassed the upper threshold for one consecutive second, the reference assistance force is increased to decrease the EMG level. As soon as the EMG is under the lower threshold, the EMG-driven controller input is shut off, making sure the assistance force is not increasing anymore. This is repeated 5 times during the calibration phase, after which the reference force of 42 Newton is reached. The rest of a few seconds in the lower position concludes the calibration phase.

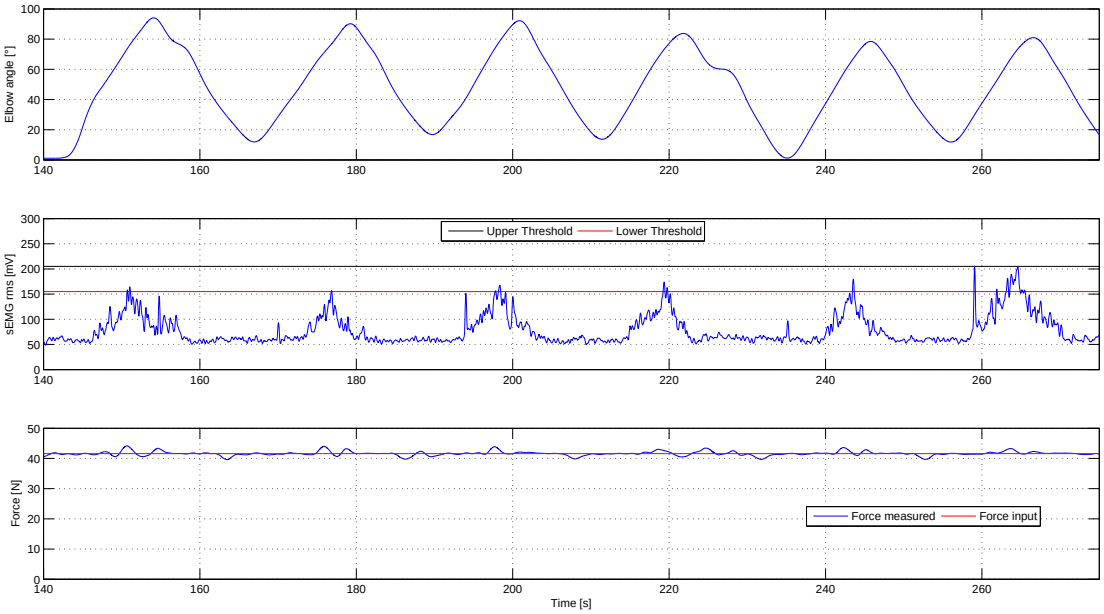

Figure 5.4: The execution phase of the experiment for subject A.

In the second phase, shown in Figure 5.4 and starting from 140 seconds, the lifting task is repeated, but now without a break in the upper position. As can be seen from the EMG plot, the EMG is now limited to the upper threshold, which refers to lifting a 0.5 kg load in constant position as set during the threshold calibration experiment. This limitation achieves the goal as set in the introduction Chapter 1. By not going above the upper threshold in the remainder of the experiment, the assistance force does not need to increase anymore. The reference force therefore remains constant. However, the measured force is not equal to the reference assistance force. This error in the following behavior is caused by two main factors. First, the TSA force controller has a low bandwidth and controls slowly. Second, the measured force is disturbed by the movement of the arm. When raising the arm, the tension on the string is reduced, decreasing the measured force. When lowering the arm, the force on the string is increased, which also increases the measured force. When moving in a rapid way, the force disturbance is applied faster than the force controller can compensate for. Therefore the following behavior from the force control contains some errors.

In the second phase also some undesired behavior appeared for subject A. Around 225 seconds, the subject got stuck in the position, as the TSA module did not allow the subject to go down. This behavior is caused in this situation due to the movement speed of the subject, which is faster than the system allows in the current configuration. When the subject moves too fast, the force control lags behind, increasing the integral action significantly in the process. This integral action first needs to be removed before the string will twist in the other direction. However, for the current system this has not been improved.

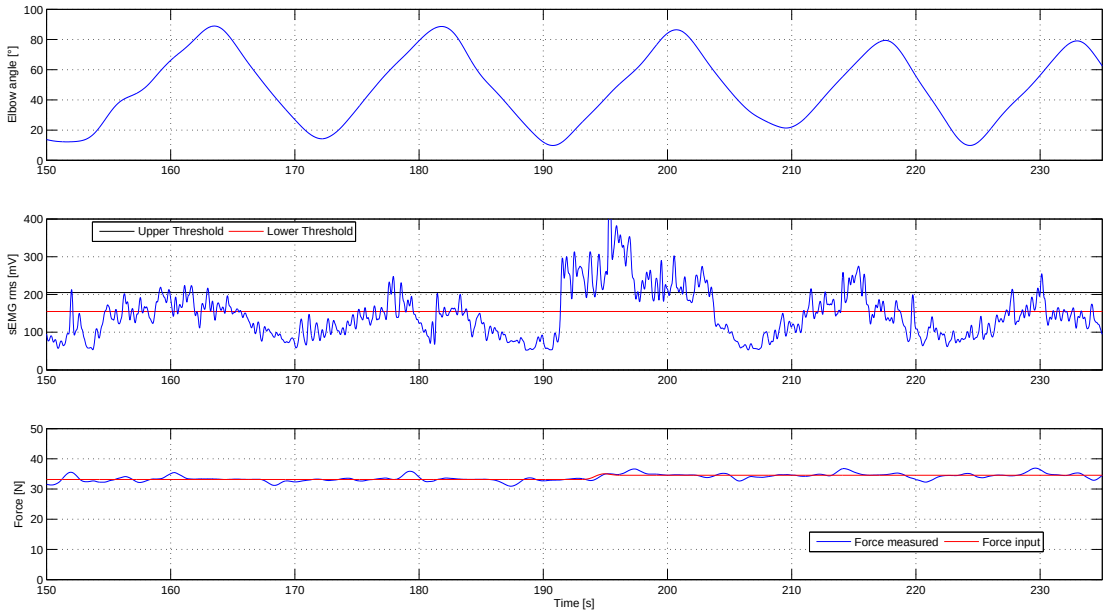

Figure 5.5: The execution phase of the experiment for subject B.

Next to the previously described behavior also some other behavior could be noticed at other subjects. For example, an observation in the execution phase of subject B, which is shown in Figure 5.5, is the increase in assistance during the execution phase. For the third iteration of the lifting task at 195 seconds, the EMG values increase above the upper threshold, and some additional assistance is needed. The increase in EMG signal could be caused due to a supination movement, as the EMG is sensible for this type of movement as well. This extra assistance force is added during this iteration and will also be used in the next iterations, as can be seen in the figure. The control strategy is still active during the execution phase, though the extra assistance will not be activated if it is not needed. This results in an adaptable controller.

Furthermore, differences in EMG values could be noticed between subjects and between sessions with the same subject. Next to that, the EMG values significantly changed according to the

pronation-supination position of the lower arm. If the arm is totally supinated, the EMG values measured are highest, since the biceps also play a role in this movement. Therefore during the experiments some extra attention is paid to make sure the experiments are executed with the same level of supination for each subject and each session. Also the position of the arm as well as the movement speed could cause for different EMG behavior. When the arm is further towards the upper position, the muscle is more contracted, which changes the torque arm as well. A higher movement speed requires a larger acceleration and force, which increases the EMG.

5.3 Limitations

Next to the desired behavior also some undesired behavior occurred. During experiments sometimes the movement was blocked when moving down. This blocking was possibly caused by two things: the errors in the force control following behavior and the slow integrator in the EMG-driven control strategy. When the error in the force control causes for a too low force, the controller wants to compensate the error. But when the movement is switching from upwards to downwards, the force on the string will increase due to the static friction when starting the movement. This increases the error, causing the TSA module to twist harder in the opposite direction of the new downwards movement.

The slow integrator in the EMG-driven control strategy is the second possible cause for the blocking behavior. When the movement is going too fast, the controller cannot keep up with the movement. This is partially caused by the delay of 1 second that is used to determine the switching behavior, which is implemented because of the variations in the EMG signal. When changing the direction this causes the TSA module to twist in the opposite direction of the movement, blocking the movement. The EMG-driven controller does not show the problem when turning around the direction of the movement slowly.

The speed of the movement is limited by the above problem, as well as the limited twisting rate of the DC motor that is used. Next to that, the resolution of the force sensor is quite inaccurate, possibly causing problems in accurately following the reference force. The movement is limited to about 90 degrees, since otherwise a longer string would be needed, which causes problems in making the device wearable.

5.4 Conclusion

In this Chapter the control strategy has been experimentally evaluated for four subjects. One subject is treated in detail in this chapter, where the other three subjects are treated in Appendix C as the results were similar. The results show that the control strategy reaches the goals set, but that there are some limitations to the setup and the control strategy. In the next chapter some final conclusions will be drawn along with some recommendations for future work.

6 Conclusion and Recommendations

6.1 Conclusion

To find out if EMG could be limited with the use of the TSA-module, first some knowledge about the muscles and the actuator was needed. By controlling the actuator using force control the TSA-module was made controllable, after which an EMG-driven control strategy could be exploited. This strategy has been tested on four different subjects by means of an experiment on the designed setup. This experiment resulted in some desired and undesired behavior.

The objective set in the introduction was to limit the muscle activity during a lifting task by using the TSA module as an assistive device. In this report the controllers used to achieve this goal have been presented. The objective is experimentally evaluated using a 2 kg load and the results show for different subjects that the EMG has been limited to the muscle activity of 0.5 kg.

Next to that, a control strategy is used that makes use of only a short calibration to set the controller variables. After that, the control strategy is able to calibrate during movements, increasing the help that is needed in order to limit the EMG to the muscle activity of a smaller load. This control strategy makes use of a short calibration, making the system easily adaptable to different users, as is shown using four different subjects: for all four subjects the muscle activity was limited to the muscle activity with a load of 0.5 kg.

When comparing the results to literature, the major difference is in the goal that has been set for this project. In [4] for example, the goal is to reduce the muscle activity EMG, without specifying how much the activity should be reduced. In this project the goal is stated more clearly by limiting the EMG to a predefined value, in this case the muscle activity of lifting a 0.5 kg load. This results in a different type of control, which is more focused at reducing the EMG compared to a preset value, where [4] uses a gain on measured EMG level to determine the direction and amplitude of the assistance force, not really controlling the EMG.

The proposed control method does not make use of complex dynamic models, since it is hard to properly estimate the joint torques from the EMG signal and the behavioral reaction of the user cannot be properly modeled. By not using a complex model but a more direct control method, this method is more adaptable to different users since less parameters need to be set or calibrated for different users. This results in a more appropriate solution for rehabilitation purposes.

In this project the calibration is done in a numeric way with a semi-automatic procedure, whereas [4] allows the subject to tune the assistance to an level of support they feel comfortable at. Calibrating in a numeric way is more reproducible, improving the adaptability to different users of the system as a whole.

The results of this project are the first step in the further investigation of using the TSA module as an assistive device, for example for rehabilitation purposes. In this report the use of an EMG-driven control strategy is presented with experimental results. There might be other solutions that will not limit the usability of the system as much, since the control strategy limits the usability to lifting only constant or increasing loads. Other solutions might improve on this point in future work.

6.2 Recommendations

The material of this report shows room for improvement in the future. First, the EMG acquisition device made by the Electrical Engineering department was very fragile and broke down quite some times. Also, the measured EMG from the device is somewhat dependent on the charge state of the batteries, as the signal was stronger when the batteries were full of charge. When multiple channels were used, very often cross-talk between channels was visible in the measurements, causing for troubles if multiple muscles were to be checked at once. One recommendation for future work would be to use a different EMG acquisition device, made by industry with more accurate tolerances, as this would improve the gathered EMG signal, making the system as a whole more reactive to the actual muscle activity.

The controller for the TSA module is a controller with only a bandwidth of 1.7 Hz, which is quite low. By using a different DC-motor with a faster turn rate, the system can be controlled faster and the performance would significantly increase. This might also reduce the problem of getting stuck when changing direction, as the force control would be better. Another improvement would be in the force sensor of the TSA module, as the resolution of 0.98 N is quite inaccurate, to increase the performance of the force control.

Using the antagonist muscle as well as the agonist muscle could also improve the control in total. When a load is applied on the arm, both muscles tend to contract to increase the total stiffness of the arm to keep it in position. By supporting both the agonistic and the antagonistic muscle the total muscle activation of both muscles could be reduced, making more assisted movement possible than only the lifting of a load.

The TSA module can also be used for other limbs, such as fingers, to assist the muscles that cause for them to move. For this a smaller string can be used, as well as a smaller DC-motor. Since the muscles in the lower arm are more densely packed, the sEMG method might not be the best solution anymore. When a muscles is located underneath another muscle indwelling EMG should be used.

Finally, the TSA module should be fixed to the back of the subject due to the long strings. To do this, the strings need to be bent, introducing a little different twisting behavior. Further research should be done into this phenomenon, after which some testing with the TSA module fixed on the back of the user can be done.

A Muscle Modeling

This chapter of the appendix is based on information from [13].

A muscle can only produce tensile forces. The muscle contraction can be modeled. A model can predict the tension in the muscle based on some input stimulation. The model can be build up from basic elements, such as the spring and dashpot. These elements can be both linear or nonlinear. In addition, the model requires an active generator of the tensile forces. By combining the basic elements in series or parallel, different properties can be achieved. Four models will be considered and reviewed on their pros and cons. Three of the models are shown in Figure A.1.

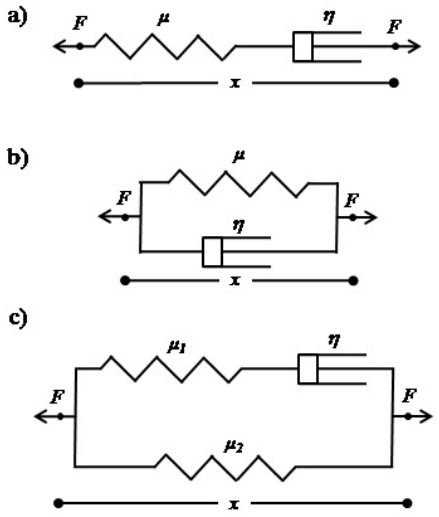

Figure A.1: Three muscle models. a) Maxwell b) Voigt c) Kelvin
[14]

A.1 Maxwell Model

The Maxwell model consists of a spring and a dashpot in series. The properties are that the forces are equal in the spring and dashpot, and the total displacement is the sum of the two displacements. For a constant load response, the displacement solution results in

$$x(t) = \frac{F}{b}t + \frac{F}{k}. \tag{3}$$

There is an initial deformation, but the deformation will increase linearly, implying that the deformation will go on forever. When the force is removed, a residual deformation exists, which suggest that the Maxwell model is not a good model under a constant load, except when time t is small.

In the constant deformation response, the force solution results in

$$F(t) = kxe^{-\frac{t}{\tau}}. \tag{4}$$

In the long term, the force decays to zero, which is not a good representation of the physiological tissue.

A.2 Voigt Model

The Voigt model consists of a spring and a dashpot in parallel. The properties are that the displacement is equal in the spring and the dashpot, and the total force is the sum of the two forces. For a constant load response, the displacement solution results in

$$x(t) = \frac{F}{k}(1 - e^{-\frac{t}{\tau}}). \tag{5}$$

In the long time period, the solution seems good, as the displacement reaches an asymptote when t goes to infinity. However, the instantaneous deformation from the Maxwell model is not present.

For the constant deformation response, the force solution results in

$$F(t) = kx. \tag{6}$$

The relationship between F, $\dot{F}$, x and $\dot{x}$ is correct. However, at $t = 0$ an infinite force is needed for an instantaneous deformation. Since this leads to a discontinuous nature of the force response, this model is also not entirely correct.

A.3 Kelvin Model

The Kelvin model combines the elements from the previous two models that are needed to describe the proper relationships. The Kelvin model consists of a spring in series with a dashpot, that is in parallel with another spring. The spring in series with the dashpot is needed for the instantaneous behavior, where the spring in parallel provides the correct long term response. The differential equation of the Kelvin model is [14]

$$F + \frac{b_1}{k_1}\dot{F} = k_0(x + \frac{b}{k_0}(1 + \frac{k_0}{k_1})\dot{x}). \tag{7}$$

A.4 Hill Model

The Hill model is a Kelvin model with in addition a force generator to account for the tension produced by contractile proteins. The force generator works in parallel with the damper to represent the contractile component of a muscle. Another difference is that the elements used in the model need not necessarily be linear elements. Nonlinear springs are typically used to represent parallel elastic elements and series elastic elements.

B TSA Force Control

In this appendix the feedback loop used in the TSA force control is shown. The plant in Figure B.1 is implemented in Simulink with an S-function that communicates with the Arduino module of the TSA module, as shown in Figure 3.5.

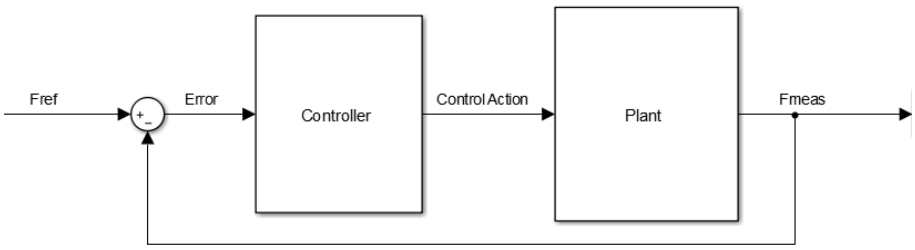

Figure B.1: The control scheme of the TSA Force Control.

C Results other subjects

In this appendix the results of subjects B, C and D are presented, as they are similar to the results of subject A. For subject B this has resulted in the EMG-driven controller with a proportional gain of 0.001 and an integral gain of 0.01. The threshold calibration plot from the 0.5 kg load static experiment is shown in Figure C.1. Similar thresholds to subject A are used, as the EMG behaves in a similar way and the mean value and the standard deviation are comparable.

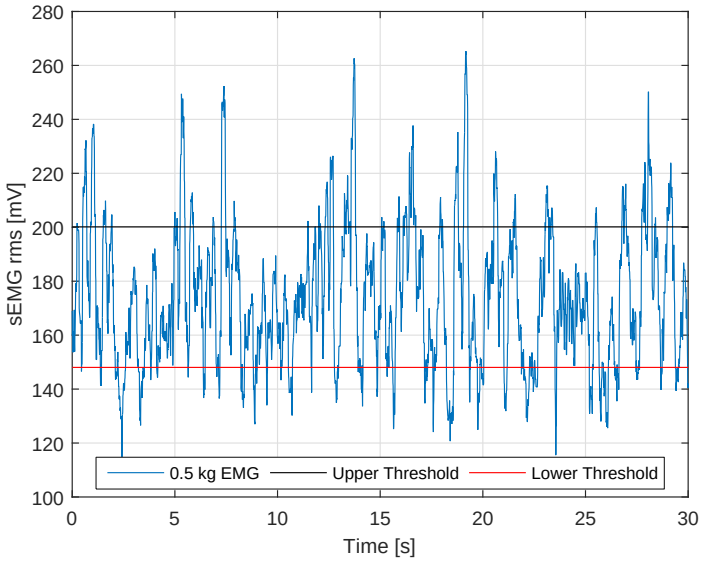

Figure C.1: The thresholds for subject B, determined using the 0.5 kg load calibration experiment.

The thresholds together with the controller parameters have been applied during the experiment. This is has resulted in the calibration phase plots of Figure C.2. Here the calibration is finished after 5 iterations, reducing the EMG to about the upper threshold and therefore the behavior with 0.5 kg. The calibrations are completed in respectively 6 and 5 iterations.

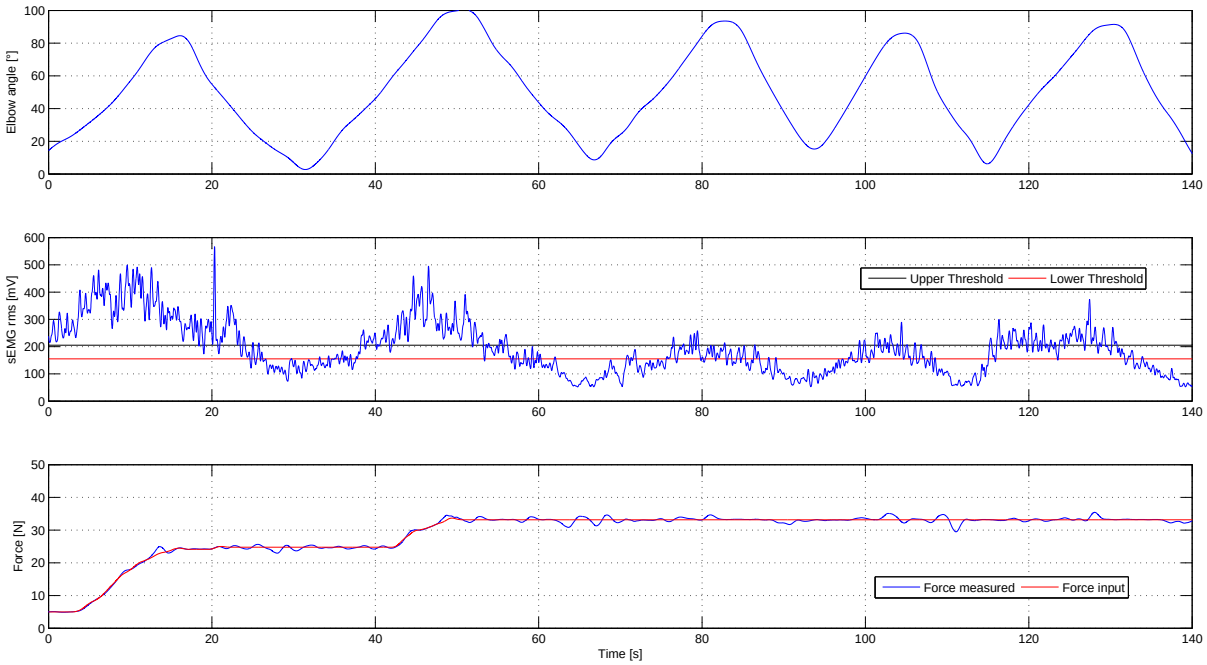

Figure C.2: The calibration phase of the experiment for subject B.

In Figure C.3 the execution phase of the experiment for subject B is shown. At the third iteration at 195 seconds the controller is needed to increase the assistance force, since the EMG is significantly over the upper threshold. This situation has been discussed in further detail in Chapter 5.

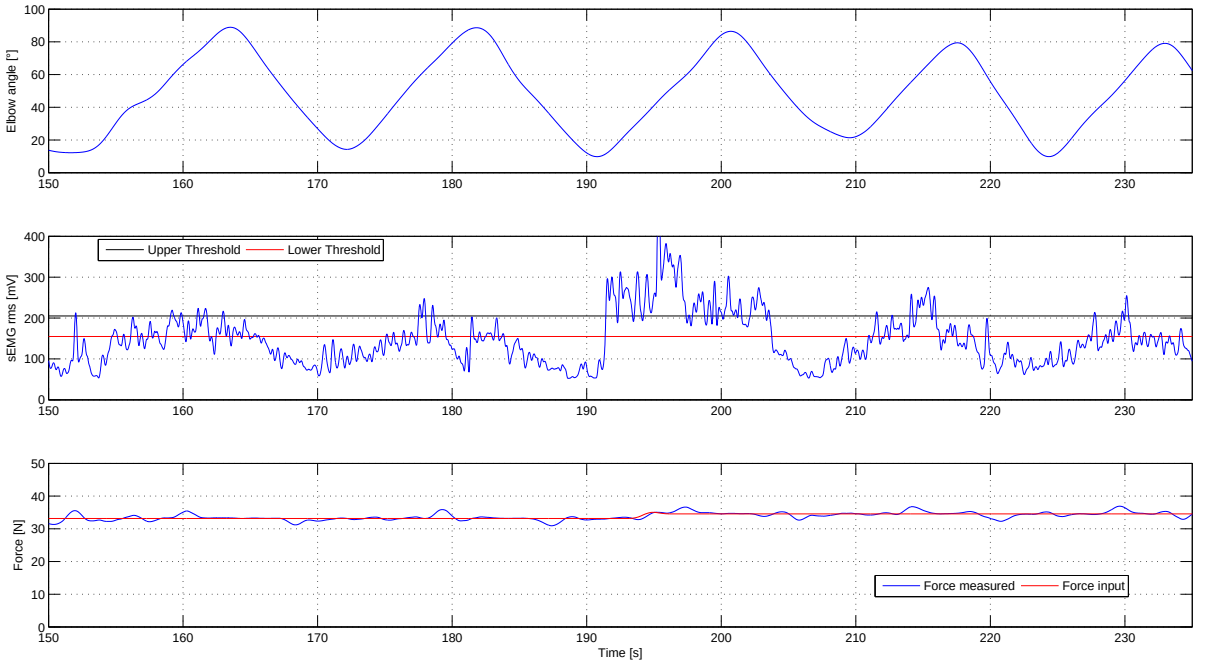

Figure C.3: The execution phase of the experiment for subject B.

For subject C and subject D the results are similar as well. The thresholds are chosen lower, since the muscle activity EMG values were lower compared to subject A and B. The threshold calibration plots are shown in Figures C.4 and C.5. The controller used for subject C has a proportional gain of 0.01 and an integral part of 0.1. The controller used for subject D has a proportional gain of 0.01 and an integral part of 0.4. This lead to the results from Figures C.6, C.7, C.8 and C.9. These results are very similar to the previous results, validating the adaptability of the control strategy and the system as a whole to different subjects.

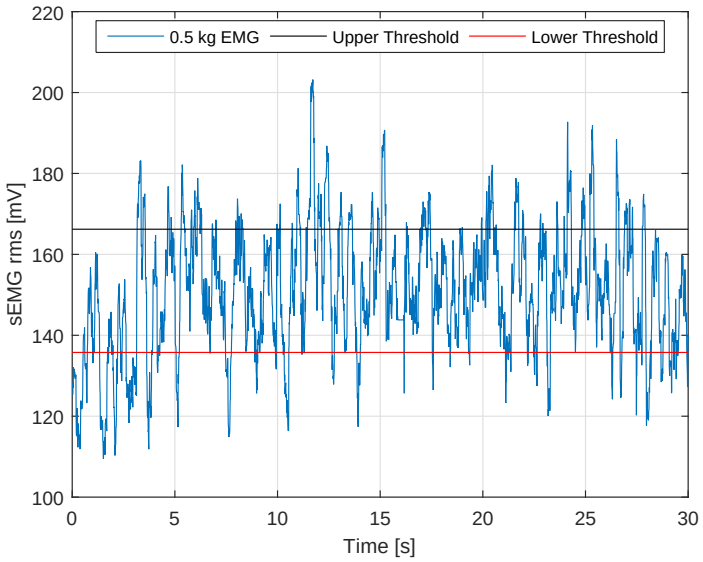

Figure C.4: The thresholds for subject C, determined using the 0.5 kg load calibration experiment.

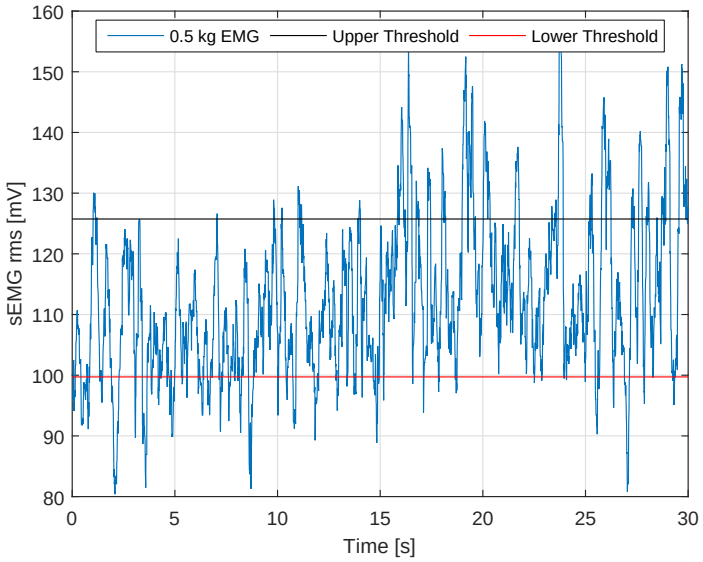

Figure C.5: The thresholds for subject D, determined using the 0.5 kg load calibration experiment.

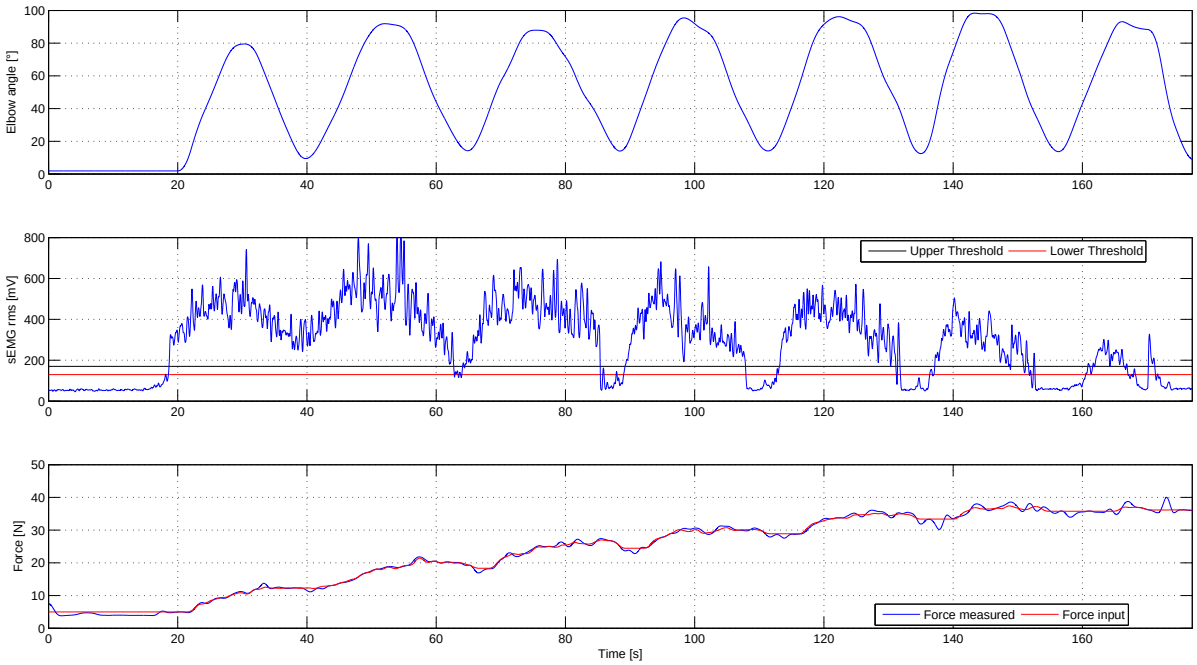

Figure C.6: The calibration phase of the experiment for subject C.

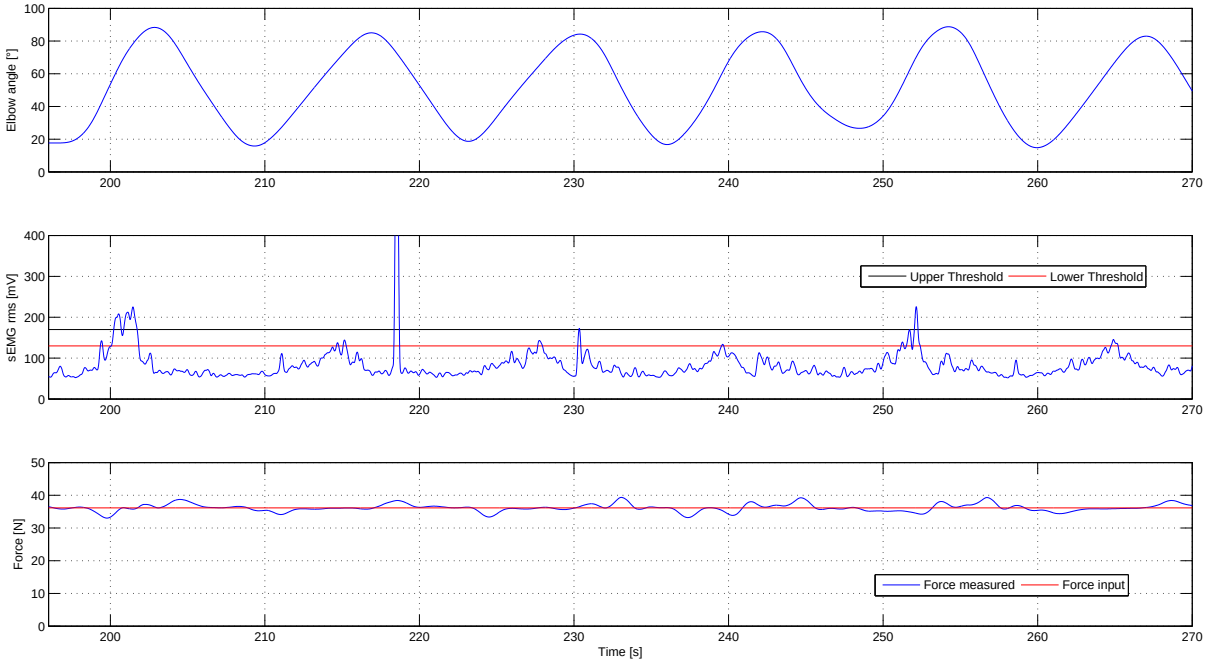

Figure C.7: The execution phase of the experiment for subject C.

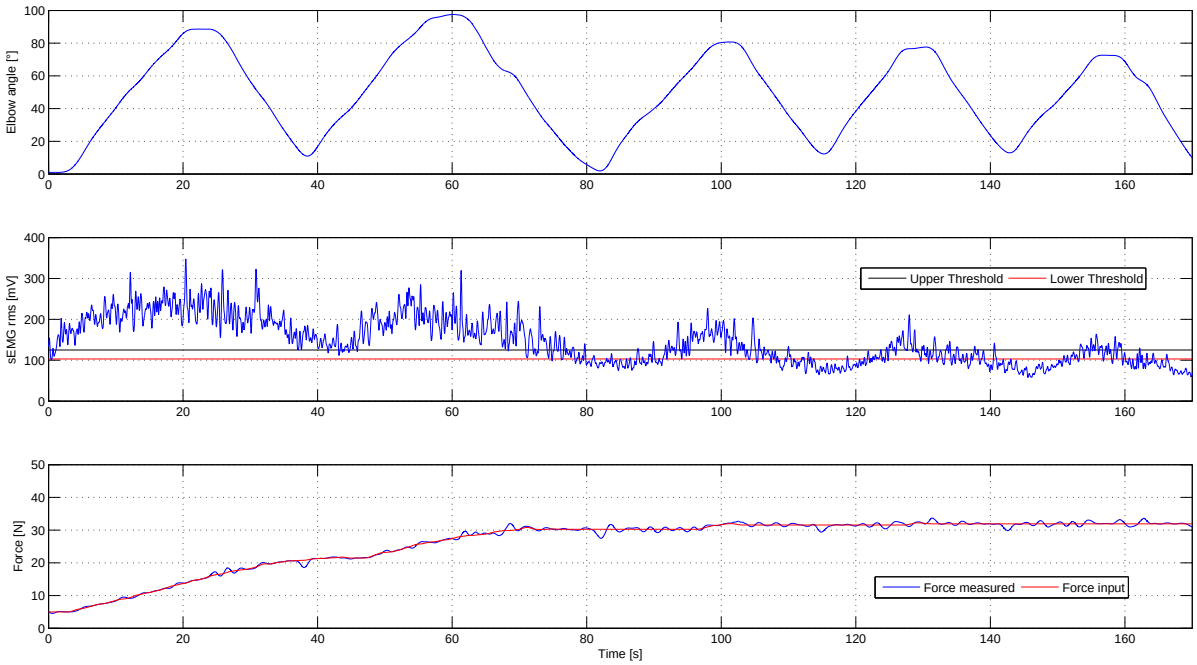

Figure C.8: The calibration phase of the experiment for subject D.

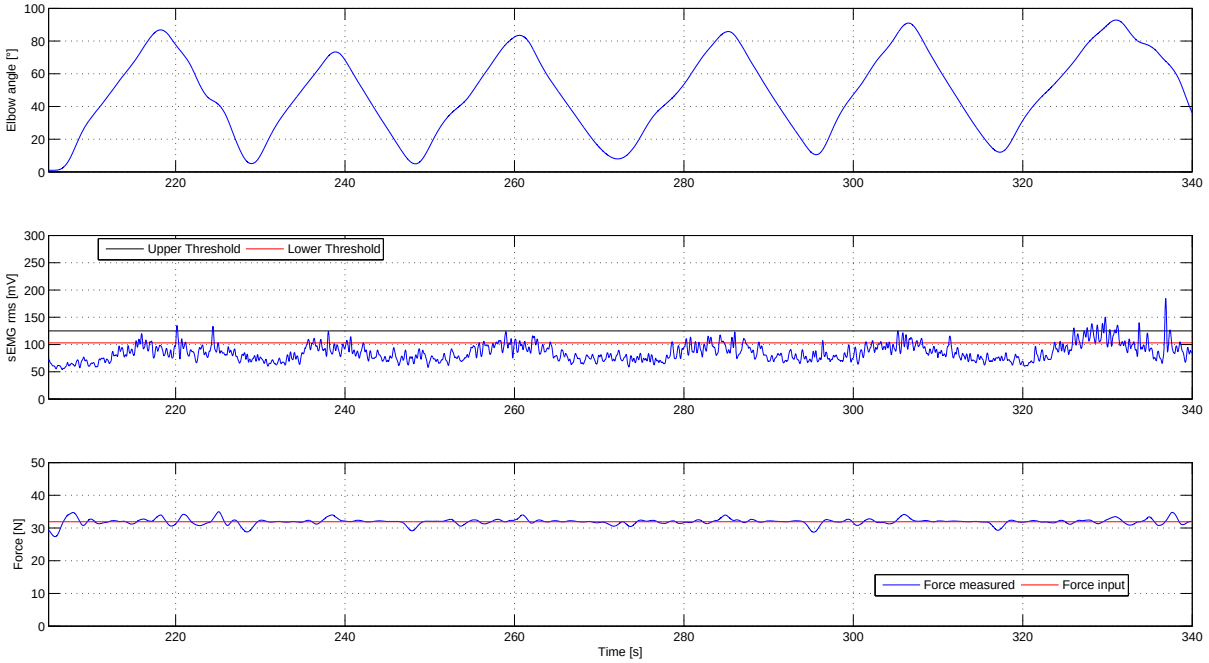

Figure C.9: The execution phase of the experiment for subject D.

Bibliography

[1] J.C. Perry, J. Rosen, S. Burns (2007), *Upper-Limb Powered Exoskeleton Design*, International Journal of Humanoid Robotics Volume 4, Issue 3, September 2007, Pages 529-548

[2] T. Nef, M. Mihelj, R. Riener (2007), *ARMin: a robot for patient-cooperative arm therapy*, Medical & Biological Engineering & Computing, September 2007, Volume 45, Issue 9, pp 887900

[3] N.G. Tsagarakis, D. G. Caldwell (2003), *Development and Control of a 'Soft-Actuate' Exos*, Autonomous Robots 15, 2133, 2003

[4] T. Lenzi, S.M.M. De Rossi, N. Vitiello, M.C. Carozza (2011), *Proportional EMG control for upper-limb powered exoskeletons*, 33rd Annual International Conference of the IEEE EMBS, Boston, Massachusetts, USA

[5] R.W. Norman and P.V. Komi (1979), *Electromechanical delay in skeletal muscle under normal movement conditions*, Acta physiologica Scandinavica, vol. 106, Jul. 1979, pp. 241-8.

[6] K. Kiguchi, S. Kariya, K. Watanabe, K. Izumi, T. Fukuda (2001),*An Exoskeletal Robot for Human Elbow Motion SupportSensor Fusion, Adaptation, and Control*, IEEE Transactions on systems, Man, and Cyberneticspart B: Cybernetics, Vol. 31, No. 3, June 2001

[7] R. Song, K.Y. Tong (2005), *Using recurrent artificial neural network model to estimate voluntary elbow torque in dynamic situations*, Med. Biol. Eng. Comput., 2005, 43, 473-480

[8] J. Rosen, M. Brand, M. Fuchs, and M. Arcan (2001), *A myosignal-based powered exoskeleton system*, IEEE Trans. Syst.,Man, Cybern., vol. 31, no. 3, pp. 210222, May 2001.

[9] M. Hosseini, R. Meattini, G. Palli and C. Melchiorri (2016,under review),*A Wearable Robotic Device Based on Twisted String Actuation for Rehabilitation and Assistive Applications*,

[10] D.A. Winter (2009). *Biomechanics and Motor Control of Human Movement*, fourth edition, USA, John Wiley & Sons Inc.

[11] C. J. De Luca, A. Adam, R. Wotiz, L. Donald Gilmore, S. Hamid Nawab (2006), *Decomposition of Surface EMG Signals*, Journal of Neurophysiology, 1 September 2006 Vol. 96 no. 3, 1646-1657

[12] G. Palli, C. Natale, C. Mat, C. Melchiorri, T. Würtz (2013), *Modeling and Control of the Twisted String Actuation System*, IEEE/ASME Transactions on Mechatronics, Vol. 18, No. 2, April 2013

[13] G.T. Yamaguchi (2001). *Dynamic Modeling of Musculoskeletal Motion*, first edition, USA, Arizona State University, Springer Science & Business Media

[14] R.K. Korhonen, S. Saarakkala (2011), *Biomechanics and Modeling of Skeletal Soft Tissues*, Theoretical Biomechanics, Dr Vaclav Klika (Ed.), InTech, DOI: 10.5772/19975